Solution of Bifurcation Equations for Formation Patterns in the Visual Cortex of the Brain

ALGIS GARLIAUSKAS

Laboratory of Neuroinformatics
Institute of Mathematics and Informatics
Akademijos 4, 2600 Vilnius
LITHUANIA
galgis@ktl.mii.lt

Abstract: Stripes and other forms of activity are created during early onthogenesis of the visual cortex by patterns of periodic standing waves probably based on the self-organizing dissipative ordered structures. Considering neural network theoretical principles based on an integrate-and-fire two point neurons, the N-shaped current-voltage relation was included in the model and its influence on the stability conditions were analyzed. Using theory of group and doubly-periodic kernel functions we pay main attention in search to a hexagonal lattice as the main formation for the presentation of a copying mechanism of patterns in the cortex of the brain. On the basis of reduced bifurcation equations the double and triple periodicity solutions at invariant transformations allow us to observe either repeating mosaics or global tunnels, funnels, and spiral form constants. Computation experiments were carried out as illustrative ones under different biophysical conditions of parameters, indexes of stability , angles between basic vectors of orientations, and roughly compared with the experimentally registered form constants of beings as self-organized topological structures.

Key-Words: Bifurcation equation, Stability, Group theory, Hexagonal structure, Pattern, Visual cortex.

1 Introduction

The most of the cortical areas of the brain possess the expressed layered organization with ordered topological structures. This fundamental feature of the topological structures in the primate neostriatum have oriented properties [9] and form cell islands and matrix [7] which, as it has been recently established, are present in a less visible form in all mammals. The cortical areas possess the matrix rather than the island neuronal organization. The visible clustering of the neurons indicates some boundaries of the mosaic configurations. The human and some primate neostriatum neurons, in contrast to most other animals, are laid out by clustered formations with a higher and lower cell density [21].

Another aspect of an ordered self-organized neuronal structures is bound up with the peristimulus inhibition which is well observed in the somatosensory and visual pathways [16]. This inhibition is a result of the interaction effect of an excitatory stimulus caused by the surrounding inhibitory action and often being referred to as a "Mexican-hat" pattern [17, 18]. Although in the neocortex and small areas of the cortex, the peristimulus inhibition also takes place [6, 10], this fact was successfuly used to explain the origin of island formation [13]. However the authors of the issue [18] used the lateral inhibitory connections in their inhibition model to induce the peristimulus inhibition and to "control", as they told, the competitive model which was designated to model the peristimulus inhibition through a competition mechanism. In this way they use small hexagon patches for simulation in the cortex.

Klüver's [12] classification of "form constants" into four categories covers almost completely the set of simplified visual irregularities. We are more interested in repetitive forms such as hexagonal lattices, fretworks, honeycombs which are rather respondent to the spatio-temporal pattern copying mechanism to implement a cerebral code [1]. In concomitance we only partially attach importance to the tunnel, tunnel and spiral form constants.

The paper ends with the discussion on the experimental results of iso-orientation structures in the visual cortex of beings and artificial self-organizing dissipative ordered structures - form constants - obtained by means of the formal methodology.

2 Theoretical Principles and Models

2.1 Presentation of Neuron in Model

A neuron as the main individual element in the cortex of the brain can be represented by much differed forms of an abstraction. As usuall a neuron in artificial neural network (ANN) is presented as a single isopotential compartment - point neuron, though in reality it is spatially extended with extensively branched dendrite trees and axon arbors. We will use both cases:

first, when we go over to the modeling of massive populations of neurons, and second, when we try to evaluate conditions of stability and degeneracy in ANN. Further, the potential activation of the neuron is preferred, though a firing rate as a conversion of activation could be automatically set up, if it would be necessary.

Thus, we represent the general structure of ANN based on a complex neuron as a soma-axon-synapse-dendrite-soma chain. It is important to emphasize a strong nonlinearity phenomenon of this chain considering the main facts of nonlinearity in the complex neuron. Since, the investigations by Koike et al. [14], Lux et al. [15], Schwindt & Crill [20] on a dendritic membrane and neuron behavior theoretically and experimentally confirmed that the steady inward current related to voltage reflected a nonlinear process of activation; the mapping relation had slopes of positive and negative conductance arising from the supposed existence of the N-shaped current-voltage characteristic. The idealized characteristic measured experimentally by Schwindt and Crill [20] was presented. The respective current-voltage characteristic approximation is presented by Yoshizawa & Nagumo [22] for neuron, Gutman [8], and Garliauskas [4] for dendrite synapse as a polynomial one. We have to note that a threshold voltage as a fixed value, in the case with an excitation and inhibition, takes place in analysis bellow. It will be found in the range between excitation equilibrium potential and the resting one, and after neuron spike it places between the threshold potential and inhibition equilibrium one. This follows from a general model of an integrate-and-fire neuron.

2.2 Assumptions on the Neuron Model

A neuron as an enzymatic molecular "factory" with the surrounded infrastructure to be modelled raises problems of its super-complexity. Since this we restricted only on an electrical paradigm as the main assumption in a mathematical description of neuronal properties. Principal assumptions and the functional formal representation we formulate as follows:
(i) the evolution of u in the case of excitatory and inhibitory ionic channels of a neuron activation considered at time t is specified by the equation

$$c_n \frac{\partial u}{\partial t} = -\big(u - u_r\big) - g_e(t)\big(u - u_e\big) + g_i(t)\big(u - u_i\big), \quad (1)$$

where c_n is the neuron transmembrane capacitance, u_r, u_e, u_i are the respective resting, excitatory, and inhibitory equilibrium potentials ($u_i < u_r < u_e$), $g_e(t)$, $g_i(t)$ are excitatory and inhibitory conductances dependent on time t, respectively;
(ii) the representation of an axonal activation (zero equilibrium potentials) propagation by a simplified linear one-compartment description is based on the Hodgkin-Huxley [11] partial differential equation

$$\frac{1}{r_a} u_{xx} = c_m^{(a)} u_t + \frac{1}{r_m^{(a)}} u, \quad (2)$$

where r_a is the axonal intramembrane resistance per unit of length, c_a and $r_m^{(a)}$ are the capacitance and resistance of the axonal membrane, respectively.
(iii) the postsynaptic current, in the general case, can be presented as a multiplication

$$u_{kj} = \beta_{kj} \mathrm{w_{kj}} I_{kj}(u_j), \quad (3)$$

where u_j is the voltage in the input of neuron, β_{kj} is the absolute synaptic strength, $\mathrm{w_{kj}}$ is the weight between the kth and jth neurons.
(iv) the representation of a dendritic activation propagation by a nonlinear one-compartment description by the similar as (2) expression $\frac{1}{r_d} u_{xx} - c_m^{(d)} u_t - I(u) = 0$, where r_d is the dendritic intramembrane resistance per unit of dendrite length, $c_m^{(d)}$ is the capacitance of the membrane, and $I(u)$ is the current through the membrane resistance dependent on the potential at the input of a membrane;
(v) neuronal soma activation functions are presented as an integrated sodium and potassium current-voltage relation described by a simple Nagumo's approximation

$$I(u) = u(u^2 - 1), \quad (4)$$

where u is the transmembrane voltage.

We intend to examine a neural network formed by two basic populations of visual cortex: excitatory (E) and inhibitory (I) populations distributed on the plane space surface (x, y) represented in Fig.1.

Each neuron at the surface point (x, y) may be both excitatory and inhibitory at the same time and is connected through the connectivity matrix $\mathbf{W}$ with the respective neurons at the points by the alternate couplings among the excitatory and inhibitory neurons. The system of equations in discretized form of the surface space (x, y) can be presented

$$\frac{\partial u_k}{\partial t} = -\alpha_k u_k + \sum_{j=1}^{n} (-1)^{j-1} \beta_{kj} \mathrm{w_{kj}} I_{kj}(u_j) +$$

$$\gamma_k^{(d)} \frac{\partial^2 u_k}{\partial X^2}, j = 1, 2, \ldots, n; k = 1, 2, \ldots, m, \quad (5)$$

where α_k is the current decay rate toward the resting state, $\gamma_k^{(a)}$ and $\gamma_k^{(d)}$ are the respective axonal and dendrite conductances, n is the number of neurons in the column, and m is the number of neurons in the row of the lattice. By $(-1)^{j-1}$ the second righthand member reflects the sign that correspods to an alternation of the excitatory sign (plus), and inhibitory sign (minus), of the neuronal column. The distance fact in (3) was included in weights $\mathrm{w_{kj}}$ without probability sense. The last righthand-side member expresses only current along one-dimensional line X.

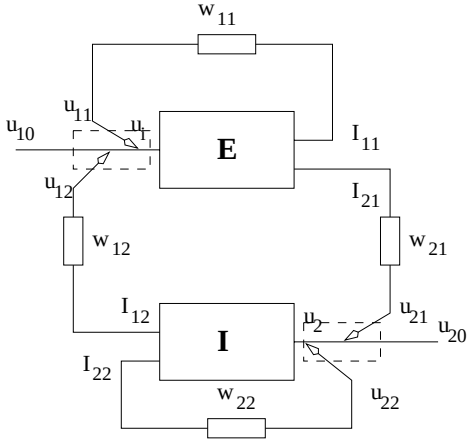

Fig. 1. Neural network with excitatory (E) and inhibitory (I) populations: dashed rectangular denotes dendrite, $I_{kj}, u_{kj}, \mathrm{w_{kj}}$ - currents, potentials,and weights in kth and jth couplings, respectively.

3 Analysis of Stability and Instability in ANN

The analysis of stability and possible degeneracy of a network system with two populations of neurons can be made basing on the standard linearization procedure of the evolutionary equations (5). In order not to complicate considerations, let us analyze a simplified case of equations (5) with only one excitatory and one inhibitory neuronal population are presented (Fig.1). Besides, we include a small parameter λ for changes of excitability, i.e., instead of β_{11} $\lambda\beta_{11}^{'}$, and instead of β_{21} $\lambda\beta_{21}^{'}$ Two equations are presented as follows

$$\left.\begin{array}{l} \frac{\partial u_1}{\partial t} = -\alpha_1 u_1 + \lambda\beta_{11}^{'} I_{11}(u_1) - \beta_{12}^{'} I_{12}(u_2) + \gamma_1^{(d)} \frac{\partial^2 u_1}{\partial X^2} \\ \frac{\partial u_2}{\partial t} = -\alpha_2 u_2 + \lambda\beta_{21}^{'} I_{21}(u_1) - \beta_{22}^{'} I_{22}(u_2) + \gamma_2^{(d)} \frac{\partial^2 u_2}{\partial X^2}, \end{array}\right\} \quad (6)$$

where $\beta_{kj}^{'} = \beta_{kj}\mathrm{w_{kj}}$ as $k, j = 1, 2$ and return to previous β_{11}, β_{21} without the mark " ' ", $u_k = \sum_{j=0}^{2} u_{kj}$ for initial conditions, $u_{01} = u_{02} = 0$, $I_{kj}(u_j)$ are the approximations of type (4). The free boundary conditions of system (6) at the origin $X = 0$, and the end of dendrites $X = S$ are given

$$\left.\begin{array}{l} \frac{\partial u_k}{\partial X}|_{X=0} = 0 \\ \frac{\partial u_k}{\partial X}|_{X=S} = 0. \end{array}\right\} \quad (7)$$

The system of partial differential equations (6) is similar to diffusion ones and the coefficients $\gamma_1^{(d)}$ and $\gamma_2^{(d)}$ are set up as diffusion coefficients for excitation and inhibition potentials whose changes are insignificant and sufficiently smooth.

The system at fixed points and taking into account a steady state condition becomes as follows

$$-\alpha_k u_k + \lambda\beta_{k1} I_{k1}(u_1) - \beta_{k2} I_{k2}(u_2) = 0, \quad k = 1, 2. \quad (8)$$

After replacing $I_{kj}(u_j)$ by polynomial approximations (4), it is not difficult to get convinced that the rest point of neurons will be the equilibrium point of the system (1). Let us denote it as the point $(u_1^*, u_2^*) = (0, 0)$. Let , $u_k = u_k^* + v_k$, where v_k is the perturbation of the equilibrium state u_k^*. Then, after the linearization of (6) and substituting u_k, we obtain a system of linearized equations regarding the variable v_k as follows

$$\left.\begin{array}{l} \frac{\partial v_1}{\partial t} = a_{11} v_1 + a_{12} v_2 + \gamma_1^{(d)} \frac{\partial^2 v_1}{\partial X^2} \\ \frac{\partial v_2}{\partial t} = a_{21} v_1 + a_{22} v_2 + \gamma_2^{(d)} \frac{\partial^2 v_2}{\partial X^2}, \end{array}\right\} \quad (9)$$

where $a_{kj} = \frac{[\partial \mathrm{W_k}(u_1, u_2)}{\partial u_j}]|_{u_j = u_j^*}$, and $\mathrm{W_k}(v_1, v_2)$ are left hand sides of the system (8).

Let us seek a solution under the wave superposition

$$v_k = \exp\{p_k t + i\omega X\}, \quad (10)$$

where p_k are roots of the charakteristic equation, $\omega = \frac{2\pi}{\Lambda}$ is the wave number and Λ is a respective wave length.

The system of equations (9) was transformed to one second order differential equation. After substituting solution (10) into ordinary equation, the characteristic equation follows of the form

$$Det(p) = \left\| \begin{array}{cc} (a_{11} - p - \gamma_1^{(d)} w^2) & a_{12} \\ a_{21} & (a_{12} - p - \gamma_2^{(d)} w^2) \end{array} \right\| = 0 \quad (11)$$

or after opening (11), we get the following second order characteristic equation

$$p^2 + [w^2(\gamma_1^{(d)} + \gamma_2^{(d)}) - (a_{11} + a_{22})]p + det(a_{ij}) - w^2(a_{11}\gamma_2^{(d)} + a_{22}\gamma_1^{(d)}) + \omega^4\gamma(d)_1\gamma_2^{(d)} = 0, \quad (12)$$

where $det(a_{ij}) = a_{11}a_{22} - a_{12}a_{21}$.

The roots of the polynomial equation (12) are

$$p_{1,2}(w^2, \lambda) = -\frac{B}{2} \pm \frac{1}{2}\sqrt{B^2 - 4C}, \quad (13)$$

where $B = w^2(\gamma_1^{(d)} + \gamma_2^{(d)}) + (a_{11} + a_{22}) + \omega^4\gamma(d)_1\gamma_2^{(d)}$, $C = det(a_{jk}) - w^2(a_{11}\gamma_2^{(d)} + a_{22}\gamma_1^{(d)})$ and after substituting of the linearized values of (4) we obtain

$$det(a_{ij}) = \left\| \begin{array}{cc} -\alpha_1 - \lambda\beta_{11} & \beta_{12} \\ -\lambda\beta_{21} & -\alpha_2 + \beta_{22} \end{array} \right\|. \quad (14)$$

The rest state $u_k(0, 0)$, in some area of the bifurcation parameter λ, is stable if and only if : (i) absolute stability if $Rep_k(w^2, \lambda) < 0$; (ii) reciprocally dissipative structures if $Rep_1(w^2, \lambda) = 0$, $Rep_2(w^2, \lambda) < 0$; (iii) periodic solutions if $Rep_1(w^2, \lambda) = Rep_2(w^2, \lambda) = 0$.

Stability may be lost at some values λ. The limit values of $p_1(w^2,\lambda)$ will be at points $p_1^-(w^2,\lambda)=0$ and

$$p_1^+(w^2\lambda)=0$$

and states will be unstable in the range

$$w_-^2 < w^2 < w_+^2.$$

$w_\pm^2$ is found from the following conditions:

$$Rep_1(w^2,\lambda)=0$$

and it may happen when $C=0$ in (13). Then $w_\pm^2 = \frac{1}{2\gamma_1^{(d)}\gamma_2^{(d)}}\{a_{11}\gamma_2^{(d)}+a_{22}\gamma_1^{(d)} \pm$

$$\left[\left(a_{11}\gamma_2^{(d)}+a_{22}\gamma_1^{(d)}\right)^2 - 4\gamma_1^{(d)}\gamma_2^{(d)}det(a_{ij})\right]^{\frac{1}{2}}\} \qquad (15)$$

and for respective λ_0 the range $[w_+^2, w_-^2] \to w_0^2$ or it follows from the condition that $\left(a_{11}\gamma_2^{(d)}+a_{22}\gamma_1^{(d)}\right)^2 = 4\gamma_1^{(d)}\gamma_2^{(d)}det(a_{ij})$. This case corresponds to so called Turing's bifurcation. For our computation example, we have got with a decrease of λ's curves shift to the left and the real eigen values become almost all negative. Among all λ one is the critical value denoted λ_0 to which respective w_0^2 corresponds.

4 Hexagonal Lattice Group Action

4.1 Hexagonal Lattice Representation

We concentrate our attention on the hexagonal lattice as the main formation for the presentation of a copying mechanism of patterns in the cortex of the brain. As to other form constants (square, rhombic) one should refer to [2, 3, 19, 21]. We assume that the basis vectors $\vec{\omega_1}$ and $\vec{\omega_2}$ satisfy to the condition $\mid\vec{\omega_1}\mid = \mid\vec{\omega_2}\mid = \omega_0$. The angle between two basis vectors is denoted as γ for the symmetry lattice. The hexagonal symmetry group scheme is presented in Fig.2 and the listing of elements is given in Table 1.

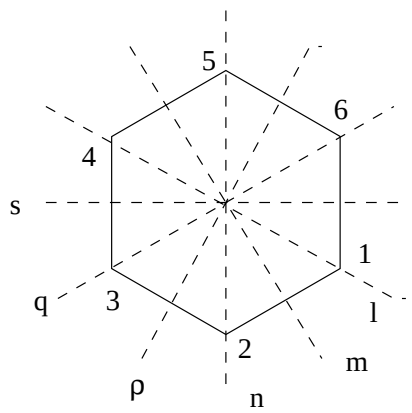

Fig. 2. The basic hexagonal symmetry group.

Table.1. Elements of the hexagonal symmetry group.

Rotation		Reflection	
Listing of el.	Angle	Listing of elem.	Axis
$\alpha=(123$ 4 5 6)	60°	$l=(26)(35)$	l
$\alpha^2=(135)$ (246)	120°	$m=(21)(36)(45)$	m
$\alpha^3=(14)(25)$ (36)	180°	$n=(31)(46)$	n
$\alpha^4=(153)$ (642)	−120°	$p=(32)(41)(56)$	p
$\alpha^5=(654321)$	−60°	$q=(42)(51)$	q
$\alpha^6=e(iden.)$	0°	$s=(43)(52)(61)$	s

The symmetry group of a hexagon is represented as a holohedry $G(\Phi)=G_6$ with the principal angle between the two basis vectors equal to 60°. From Table 1 we can see other angle values iterating 60° and the listing of reflection elements around six possible axes. The representation of the kernels at the basis functions $\varphi_1,\varphi_2,\ldots,\varphi_6$ is as follows:
(i) for the translation

$$T_a\varphi_j = e^{i<\vec{\omega}_j,\vec{a}>}\varphi_j, \qquad (16)$$

(ii) for the rotation-reflection

$$T_r\varphi_j = e^{i<\vec{r}\vec{\omega}_j,\vec{x}>}\varphi_j. \qquad (17)$$

We omitted the proof of a irreducibility of the finite dimensional invariant subspace of the operator L because it occurs in nature mostly irreducible. The kernels for six elements of the symmetry group D_6 consist of:

$$\varphi_1(\vec{x}) = D(\lambda_0,\omega_0^2)e^{i\omega_0\vec{x}}, \qquad (18.1)$$

$$\varphi_2(\vec{x}) = \bar{\varphi}_5(\vec{x}), \qquad (18.2)$$

$$\varphi_3(\vec{x}) = \bar{\varphi}_6(\vec{x}), \qquad (18.3)$$

$$\varphi_4(\vec{x}) = \bar{\varphi}_1(\vec{x}), \qquad (18.4)$$

$$\varphi_5(\vec{x}) = T_{\alpha^2}\varphi_1 = p_0 e^{\frac{1}{2}i\omega_0(-x+\sqrt{3}y)}, \qquad (18.5)$$

$$\varphi_6(\vec{x}) = T_\alpha\varphi_1 = p_0 e^{\frac{1}{2}i\omega_0(-x+\sqrt{3}y)}. \qquad (18.6)$$

The grades of exponents (18.1), (18.5), (18.6) are set up according to concrete rotation angles and coordinates of the vector $\vec{x}$ as a scalar product.

4.2. Solutions of Bifurcation Equations

The double and triple periodicity, different variants of bifurcation solutions, various possibilities of given angles, conditions of invariant transformations allow us to observe either repeating mosaics or global tunnels, funnels, and spiral form constants.

We present bellow the possible solutions built on the basis of a hexagonal lattice.

Case (a):$\psi_1 = \psi_2 = 0; \quad \psi_2 = \sqrt{-\lambda/b}$

$$\begin{pmatrix} v_1 \\ v_2 \end{pmatrix}_a = D(\lambda_0, \omega_0^2)\vec{v}\sqrt{-\lambda/b}cos[\gamma_2+\omega_0 1/2x+\sqrt{3}/2y)] \tag{19}$$

where the vector

$$\vec{\omega}_2 = \begin{pmatrix} \omega_0 cos\gamma \\ \omega_0 sin\gamma \end{pmatrix},$$

$\gamma = 60°$, and $\vec{x} = \begin{pmatrix} x \\ y \end{pmatrix}$.

Case (b): $\psi_2 = \psi_3 = 0; \quad \psi_1 = \sqrt{-\lambda/b}$

$$\begin{pmatrix} v_1 \\ v_2 \end{pmatrix}_b = D(\lambda_0, \omega_0^2)\vec{v}\sqrt{-\lambda/b}cos[\gamma_1 + \omega_0 x], \tag{20}$$

where $\vec{\omega}_1 = \begin{pmatrix} \omega_0 \\ 0 \end{pmatrix}$.

If to take $= 90°$ (square lattice) for (19), we obtain the solution with coordinate y.

Case (c):

$$\begin{pmatrix} v_1 \\ v_2 \end{pmatrix}_c = D(\lambda_0, \omega_0^2)\vec{v}\sqrt{-\lambda/b}cos[\gamma_2 + \omega_0 y). \tag{21}$$

Case (d): $\psi_1 = \psi_2 = \psi_3 = \sqrt{-\lambda/b}$

$$\begin{pmatrix} v_1 \\ v_2 \end{pmatrix}_d = D(\lambda_0, \omega_0^2)\vec{v}\sqrt{-\lambda/2a+b}\{cos[\gamma_1 + \omega_0 x]$$
$$+cos[\gamma_2+(1/2x+\sqrt{3}/2y)]+cos[\gamma_3+\omega_0(-1/2x+\sqrt{3}/2y)]\}, \tag{22}$$

where $\vec{\omega}_3 = \begin{pmatrix} \omega_0 cos\omega \\ \omega_0 sin\omega \end{pmatrix}$ is taken for $\gamma = 120°$.

Case (e): $\psi_1 = \psi_2 = 0; \quad \psi_3 = \sqrt{-\lambda/a+b}$ is not considered as absolutely unstable. The conditions of solutions (19)-(22) were briefly characterized above.

The computational examples were taken as illustrative ones under different biophysical conditions of parameters, parameters of stability of reduced bifurcation equations, and angles between basic vectors of orientations. Cases (a), (b), and (c), solutions (18)-(20) form the mosaics of the global type called spirals (19), funnels (20), and tunnels (21). Based on equation (21) at zero angles among the basic vectors of orientations, the complex honeycomb type of mosaics were modelled on the hexagonal lattice (Fig. 9a). The peaked pyramidal mosaic with contoured lines as $v(x, y) = const$ is shown in Fig. 3b, and one element structure with rather a true form - the central positive peak and six small negative peaks around the positive one - is presented in Fig.3c.

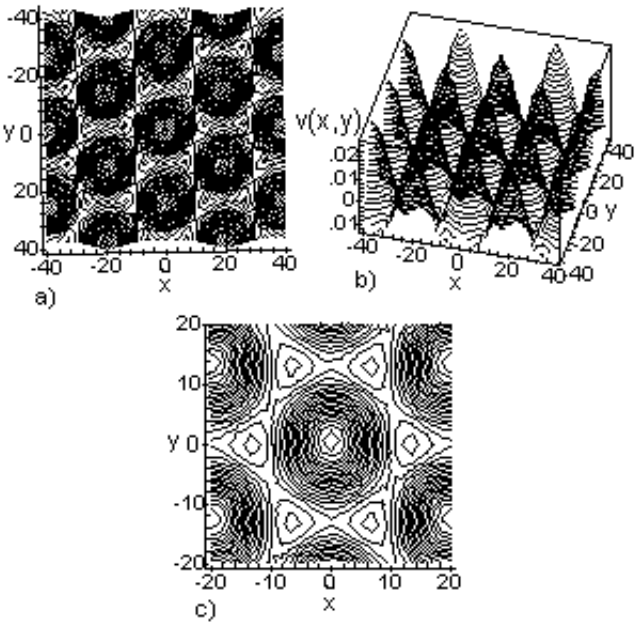

Fig.3. Honeycomb type mosaics on the hexagonal lattice. **a.** The honeycomb pattern in the plane (x, y), $\omega_0 = 60, \gamma_1 = \gamma_2 = \gamma_3 = 0$. **b.** Spatial pattern **(a)** with peaks of excitation. **c.** One element structure with equipotential lines ($v(x, y) = const$, the maximal peak in the center, minimal ones around central one).

Thus, based on the various parameter combinations and on the coupled map lattice, the different mosaic configurations as form constants have been simulated.

5 Conclusion

1. A macroscopic theoretical approach to the brain functionality corroborates that many of cells are aggregated in macrogroups which may form iso-orientation domains as stripes or blobs;
2. Stripes of activity are created during early onthogenesis of the visual cortex by patterns of periodic standing waves probably based on the self-organizing dissipative ordered structures;
3. Considering neural network theoretical principles based on an integrate-and-fire two point neurons, the N-shaped current-voltage relation was included in the model and its influence on the stability/instability conditions were analyzed , and dissipative structures established;
4. Using theory of group and doubly-periodic kernel functions we pay main attention in search to a hexagonal lattice as the main formation for the presentation of a copying mechanism of patterns in the cortex of the brain;
5.On the basis of reduced bifurcation equations the double and triple periodicity solutions at invariant transformations allow us to observe either repeating mosaics or global tunnels, funnels, and spiral form constants;

6. Computation experiments were carried out as illustrative ones under different biophysical conditions of parameters, indexes of stability , angles between basic vectors of orientations, and roughly compared with the experimentally registered form constants of beings as self-organized topological structures.

References:

[1] Calvin, W.H. (1994) The emergance of intelligence. *Sci. Am.* **271**, 89–96.

[2] Cowan, J.D. (1982) Spontaneous symmetry breaking in large scale nervous activity. *International Journal of Quantum Chemistry.* Vol. XXII, 1059–1082.

[3] Ermentrout, G.B. & Cowan, J.D. (1979) A mathematical theory of visual hallucination patterns. *Biol. Cybernetics*, **34**, 137–150.

[4] Garliauskas, A. (1998) Numeric simulation of dynamic synapse-dendrite-soma neuronal processes. *Informatica*,Vol. 9, **2**, 141–160.

[5] Garliauskas, A. (2001) The visual cortex medeling by the hexagonal topology. *Neurocomputing*, Vol. 38-40, 1229–1238.

[6] Gilbert, C. (1985) Horizontal integration in the neocortex. *Trends in Neuroscience*, **8**, 160–165.

[7] Goldman-Rakic, P.S. (1996) The prefrontal landscape: implementations of functional architecture for understanding human mentation and the central executive. *Philosophical Transactions of a Royal Society of London*, Series B, **351**,1445–1453.

[8] Gutman, A. (1991) Bistabiliy of dendrites. *International Journal of Neural Systems,* Vol. 1, **4**, 291–304.

[9] Henry, G.H., Dreher, B. & Bishop, P.O. (1974) Orientation specificity of cells in cat striate cortex. *J. Neurophysiol.* **37**, 1394–1409.

[10] Hess, R., Negishi, K. & Creutzfeldt, O. (1975) The horizontal spread of intracortical inhibition in the visual cortex. *Exp. Brain Res.* **22**,415–419.

[11] Hogkin, A.L. & Huxley, A. F. (1939) Action potentials recorded from inside a nerve fibre. *Nature*, **144**, 710–711.

[12] Klüver, H. (1967) *Mescal and the mechanisms of hallucination.* Chicago: University of Chicago Press.

[13] Kohonen, T. (1984) *Self-Organization and Associative Memory.* Berlin: Springer-Verlag, Berlin.

[14] Koike, H., Okada, Y., Oshima, T. & Takahashi, K. (1968) Accommodative behavior of cat pyramidal tract cells investigated with intracellular injection of currents. *Exp. Brain Res.* **5**, 173–188.

[15] Lux, H.D., Schubert, P. & Kreutzberg, G. W. (1970) Direct matching of morphological and electrophysiological data in cat spinal motoneurons. In *Excitatory synaptic mechanisms* (Anderson, P. & J.K.S. Jansen, J.K.S., eds), Universitets forlaget, Oslo, 189–198.

[16] Mountcastle, V. (1990) An organizing principle for cerebral Function. In *The Mindful Brain.*(Edelman, G. & Mountcastle, V. eds). Cambridge: MIT Press, 1–50.

[17] Reggia, J.A., D'Autrechy, C., Sutton, C. G. & Weinrich, M.A. (1992) Competitive distribution theory of neocortical dynamics. *Neural Computation*, **4**, 287–317.

[18] Reggia, J.A., Sutton, G.G., D'Autrechy, C.l., Cho, S. & Armentrout, S.L. (2000) Cortical inhibition as explained by competitive distribution hypothesis. In *Network Models for Control and Processing*(Fraser, M.D., ed). Portland: IntellectTM, 31–62.

[19] Sattinger, D.H. (1978) Group representation theory, bifurcation theory and pattern formation. *Journal of Functional Analysis,* **28**, 58–101.

[20] Schwindt, P. & Crill, W. E. (1977) A persistent negative resistance in cat lumber motoneurons. *Brain Res.* **120**, 173–178.

[21] Shepherd, G.M. (1990) *The Synaptic Organization of the Brain.* Oxford: Oxford Universiry Press.

[22] Yoshizawa, S., Usada, M. & Nagumo, J. (1982) Pulse generated by a degenerate analog neuron model. *Biol. Cybern.* **45**, 23–33.